Multiscale Experimental Study and Modeling of l -Glutamic acid Crystallization: Emphasis on a Kinetic Explanation of the Ostwald Rule of Stages

Yousra Tahri, Emilie Gagnière, Elodie Chabanon, Tijani Bounahmidi, Zdeněk Kožíšek, Nadine Candoni, Stéphane Veesler, Moussa Boukerche, Denis Mangin

Multiscale experimental study and modeling of L-glutamic acid crystallization: emphasis on a kinetic explanation of the Ostwald rule of stages

Yousra Tahri [1,2,6], Emilie Gagnière[1], Elodie Chabanon[1], Tijani Bounahmidi [2,6], Zdeněk Kožíšek[3], Nadine Candoni[4], Stéphane Veesler[4], Moussa Boukerche[5], Denis Mangin[1]

[1]Université de Lyon, Université Claude Bernard Lyon 1, CNRS, UMR 5007, LAGEP, 43 Boulevard du 11 Novembre 1918, 69622 Villeurbanne, France

[2] Euromed Research center, Université Euromed de Fès, Euromed University of Fes, Route de Meknes, 30000, Fès, Morocco

[3] Institute of Physics of the Czech Academy of Sciences, Cukrovarnicka 10, 16200 Praha 6, Czech Republic

[4] CINaM, CNRS, UMR 7325, Aix-Marseille Université, Campus de Luminy, F-13288 Marseille, France

[5] Process Research & Development, AbbVie Inc., 1401 Sheridan Road, North Chicago, Illinois 60064, United States

[6] LASPI, Ecole Mohammadia d'Ingénieurs, Université Mohamed V de Rabat, B.P ; 765 Rabat-Agdal, Morocco

ABSTRACT:

This work presents an experimental and a numerical study to highlight a kinetic explanation ~~to~~ of the Ostwald rule of stages (ORS). To demonstrate this explanation, L-glutamic acid (LGlu) (a monotropic system with two polymorphs) were crystallized in three different scales: Liter scale in a 2L stirred crystallizer, milliliter scale in a 4ml stagnant cell and microliter scale in microfluidic channels. Cooling crystallization experiments were performed in water at different temperature and supersaturation conditions. The LGlu polymorphic system was found to follow the ORS at low temperature (between 5°C and 30°C). However, in similar operating conditions, the stable polymorph crystallized preferentially or exclusively in the stagnant cell and in microfluidics. To explain the ORS in the stirred crystallizer at low temperature, a model based on the kinetic equation was used. By taking into account the Gibbs Thomson effect (Solubility variation with size), the simulations in the nanoscopic scale showed the dissolution of the slow-growing stable phase nuclei in favor of the fast-growing metastable phase nuclei. Consequently, the numerical results showed that the Gibbs Thomson effect is a key factor in polymorph competition and that considering this effect, in certain kinetic and equilibrium conditions, could allow explaining and simulating the ORS.

1. INTRODUCTION:

The term polymorphism denotes the ability of a substance to exist in more than one crystalline state[1]. These crystalline states have the same chemical composition but different unit cells and are called polymorphs[2]. Because of the difference in their structures, two polymorphs present different physical and chemical properties and are considered as two different solid materials[2].

At given temperature and pressure, except at the transition temperature of enantiotropic systems, only one polymorph is thermodynamically stable[3]: the polymorph with the lowest free energy. All the other polymorphs are metastable. A metastable polymorph has a higher solubility than the stable one and then has a higher bioavailability. Therefore, polymorphism control in the pharmaceutical industry is crucial in order to prevent any transformation during manufacturing and storage. Lee et al.[4] have reported many events concerning solid-state issues with polymorphism of pharmaceutical drugs. One of the main reasons why polymorphism is difficult to control is that, often, the metastable polymorph appears first. So what is the explanation behind such a behavior?

The presence of a factor (solvent nature, foreign particles) acting like a hindrance to the stable polymorph crystallization[5,6] may be the first reason behind the metastable polymorph preferential or exclusive crystallization. The second reason is the Ostwald rule of stages (ORS), which was formulated by W. Ostwald in the form[7,8] *"in the course of transformation of an unstable (or meta-stable) state into a stable one, the system does not go directly to the most stable conformation (corresponding to the modification with the lowest free energy) but prefers to reach intermediate stages (corresponding to other possible meta-stable modifications) having the closest free energy difference to the initial state"* . This rule was explained using kinetics[9–11], irreversible thermodynamics[12,13] and structural effect[13]. According to Nyvlt[9] works, if the metastable polymorph nucleation rate is very high compared to the stable one, the metastable polymorph crystallizes first according to the ORS. Cardew and Davey[10,11] have stated that using only nucleation kinetics to explain the ORS is not enough and that growth rate should also be considered. What we suggest in this work is that using nucleation and growth kinetics is still not enough and that the Gibbs Thomson effect (curvature dependence of the equilibrium concentration) [14,15] is to be considered to kinetically explain the ORS[16] . It is worth

noting that the coarsening mechanism affecting particles of a single phase and resulting from the Gibbs Thomson effect is called the Ostwald ripening.

Let's consider the crystallization from solution of a dimorphic (monotropic) system that follows the ORS. From the macroscopic point of view, what is observed, at the beginning of the crystallization process, is simply the nucleation and the growth of the metastable polymorph. What we suggest is the following: the stable and the metastable polymorphs nucleate at the same time and start to grow, inducing a decrease of the solution concentration. Let's now imagine that the metastable polymorph growths faster than the stable one. Then, the nuclei of the stable polymorph, which grow slower, will find themselves in an undersaturated solution, with respect to their size (their size becoming under the critical size after the concentration drop) and will be doomed to dissolve. Of course, this kinetic explanation of the ORS is only valid when the nucleation kinetics and mainly the growth kinetics of the metastable polymorph are several times higher than those of the stable one and when the difference between the equilibrium concentrations of the polymorphs is not too large. When the differences between the relative nucleation and growth kinetics of the two polymorphs are not significant, the system is expected to follow thermodynamics. In addition, when the metastable phase has a significantly higher solubility than the stable phase in a way that the difference in size between the polymorphs can no longer lead to a higher solubility for the clusters of the stable polymorph, then the stable polymorph is expected to remain once it nucleates.

Beside the stochastic models[17] and the molecular models[18,19] that can simulate the behavior of a system that follows the ORS, we showed in a previous work[20] that considering the Gibbs Thomson effect allowed modeling the ORS using the classical nucleation theory.

In this work, a multiscale experimental study and simulations were used to validate our explanation to the ORS involving the Gibbs Thomson effect. The product used was the L-Glutamic acid (LGlu). This amino acid has two well-known polymorphs: a stable polymorph β

shaped as needles [21] or as lozenge slabs [22] and a metastable polymorph α shaped as prisms[21]. In the experimental section, we compared the results of LGlu cooling crystallization in three different devices: a liter scale crystallizer, a milliliter scale stagnant cell and a microfluidic device. In the modeling section, we used a kinetic model that was previously built[20] to show the behavior of each LGlu polymorph at early stages of crystallization. Lastly, the experimental and the modeling works were both discussed.

2. EXPERIMENTAL SECTION:

2.1 Materials and solubility data:

In all the experiments we used ultrapure water and purchased L-Glutamic acid (chemical purity ≥ 99.5%, Sigma Aldrich). Figure 1 presents the microscope images and XRD patterns of stable polymorph β and metastable polymorph α. For more details about the solubility measurement see reference [22].

2.2 Experimental setups:

Three different devices were used to carry out LGlu crystallization in water. The first device was a stirred double jacketed vessel of 2L equipped with an *in situ* video probe and an FBRM probe (cf. Figure 2-A). The second one was a non-agitated thermostated cell of 4mL placed under a microscope (cf. Figure 2-B). More details are given in reference [22]. The third device was a droplet-based microfluidic setup composed of a droplet factory and a storage chip (cf. Figure 2-C) previously described in references[23,24] The droplet factory was composed of a PEEK-T-junction and PTFA tubings with an internal diameter of 1mm. The continuous phase and the dispersed phase were separately loaded using separate syringes placed in a syringe pump (neMESYS®). In all the experiments, the continuous phase was a fluorinated oil (Krytox® GPL 105) whereas the dispersed phase was LGlu solution. A large number of microliter scale droplets (about 0.5µL) of LGlu solution with different concentrations were generated in the Teflon channels. The channels were stored in a thermostated tubing-holder

equipped with a camera. Observation of droplet evolution was carried out using a digital camera with various zooms (Opto GmbH) attached to an XYZ motorized arm (ANACRISMAT). Thus, this camera can be programmed to memorize the position and focusing of each droplet. Finally, the camera took photos of each droplet with a pre-set time interval.

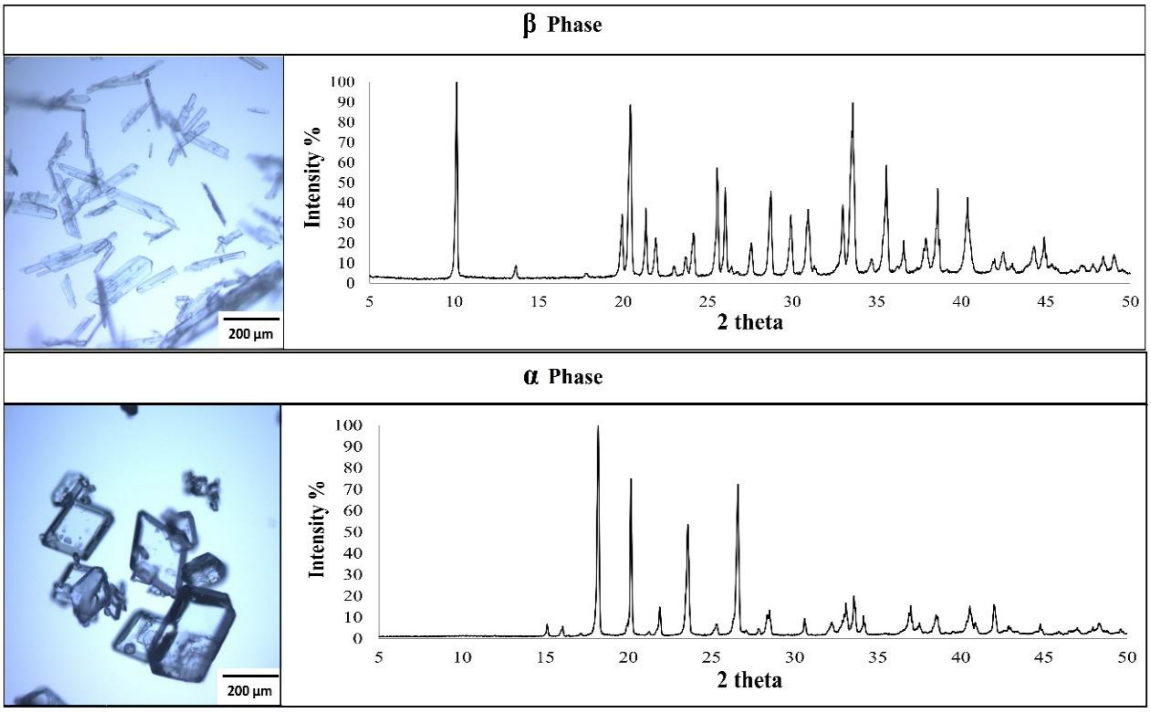

Figure 1. Microscope images and XDR patterns of α and β polymorphs

2.3 Operating conditions

Cooling crystallization of LGlu in water were performed in the three devices in order to compare and discuss the crystallization outcome in the three scales. The details about the operating conditions in the 2L crystallizer (cf. Table 1-A) and the 4ml cell (cf. Table 1-B) can be found in our previous work[22]. A cooling ramp of -1.5¨C/min was applied in both devices. In the stirred crystallizer, nucleation sometimes occurred during the cooling, while it systematically took place only after reaching the final temperature in the stagnant cell.

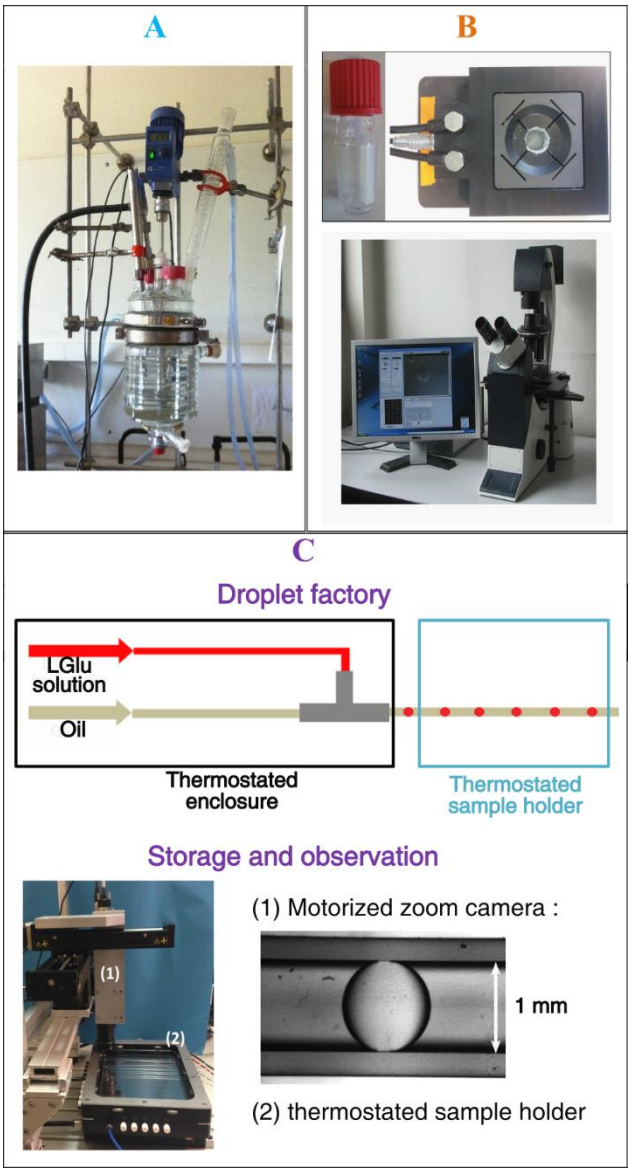

Figure 2. Experimental setups: (a) 2L batch crystallizer, (b) 4mL cell and (c) microfluidics.

In microfluidics, the microliter droplets of LGlu solution were generated at 65°C regardless of the initial concentration (cf. Table 1-C). In each microchannel, a minimum of 50 identical droplets of a given concentration was stored. All the channels were kept in the thermostated sample holder at 65°C for two hours. Afterward, the temperature of the sample holder with the channels underwent a drop to the final temperature. All the droplets were carefully observed during the cooling process. No nucleation was observed before reaching the final temperature for all the experiments.

Table 1. Operating conditions in (A) the 2L stirred crystallizer (B) The 4 mL stagnant cell and (C) the microliter droplets

	LGlu initial concentration (g/kg of solvent)	Equilibrium temperature of β (°C)	Supersaturation ratio* (calculated regarding β) S_β (-)	Final temperature (°C)
A	43	72	1.5; 3.0; 3.0	60; 40; 10
	31	61	1.7; 4.2	45; 10
	22	51	1.7; 2.2; 6.1	35; 30; 5
	15	40	1.8; 2.8; 4.2	25; 15; 5
B	43	72	3.0; 6.3; 9.0	40; 20; 10
	31	61	4.5; 6.5	10; 20
	22	51	4.6	10
C	29,1	60	2.5; 3.4; 5.4; 6.5	35; 26; 13; 8
	20,4	50	2.4; 3.8; 4.6	26; 13; 8
	14,5	40	3.2	8

*when the nucleation occurs. Spontaneous nucleation was sometimes observed before reaching the final temperature in the 2L crystallizer; in the two other devices, nucleation always occurred at final temperature after induction time.

2.4 Experimental results

Experimental results are summarized in Figure 3. The solubility of α and β are depicted with solid lines. The solubility measurement details are given in a previous work[22]. The metastable zone limit of both polymorphs in the 2L crystallizer, corresponding to spontaneous nucleation observed in certain experiments performed with that 2L crystallizer, is also represented[22]. Because of the simultaneous nucleation of both polymorphs, the metastable zone limit of each polymorph could not be distinguished. It is noteworthy that there are different markers in the graph with different shapes and colors. The colors refer to the device used in the experiments. The empty squares indicate the initial concentration and initial temperature. The full markers positions indicate the nucleation temperature just before the supersaturation drop while their

shape informs about the polymorphs observed. In the 2L crystallizer, the polymorph was first deduced by observation of its habit and was confirmed by XRD. In the microfluidic device, it was confirmed by Raman spectroscopy. For all the experiments in the stirred crystallizer, the polymorphic transition took from 6 hours to 6 days to be completed depending on the temperature.

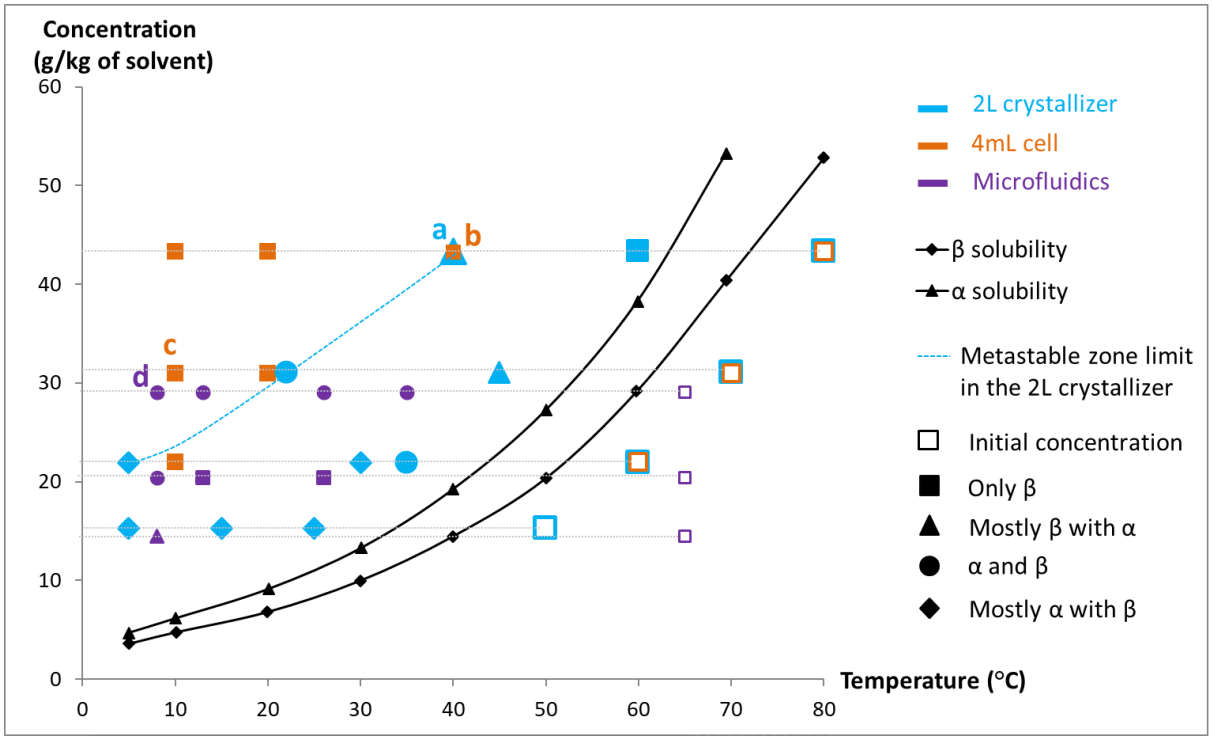

Figure 3. Crystallization domains of α and β polymorphs in the 2L crystallizer (blue), the 4ml stagnant cell (orange), and the microfluidic device (purple). The full markers denote different experiments: marker position indicates the nucleation temperature just before the supersaturation drop, marker shape informs about the polymorphs observed. Markers a, b, c, and d relate experiments detailed in the text

Let us detail 4 typical experiments, represented by points (a) (b) (c) and (d) in Figure 3:

- Experiment (a) was carried out in the 2L batch crystallizer. The initial concentration was 43g/kg of solvent and the initial temperature was 82°C; a blue empty square marks these initial

conditions in Figure 3. The solution was cooled to 40°C. Using the FBRM probe, a jump in the chord length distribution was observed once 40°C was reached. Thus, it was deduced that the nucleation occurred at 40°C, on the limit of the metastable zone, as shown by the position of the marker (a) on Figure 3. During the experiment (a), α and β were observed with a preferential crystallization of the stable polymorph β; this is represented by the *triangular* shape of the marker (a). Figure 4 shows a picture of a β crystal observed 40 minutes after the cooling start and a picture of an α crystal observed 50 minutes after the cooling start. It is worth noting that after 6 hours at the final temperature, the polymorphic transition of α to β was completed.

-Experiment (b) was carried out in the 4mL stagnant cell. The initial concentration was 43g/kg of solvent, the initial temperature was 82°C; an orange empty square marks these initial conditions in Figure 3. The solution was cooled to 40°C. The first crystals appeared after the final temperature was reached and only the stable polymorph β was observed. These results are represented in Figure 3 by an orange full square. Figure 4 shows a picture of a β crystal observed 140 minutes after the cooling start. Let us note that this crystal was first observed 10 minutes before the picture.

-Experiment (c) was also carried out in the 4mL cell. However, the operating conditions were different. Since the supersaturation was higher ($S_\beta = 6.5$ for the experiment (c) while $S_\beta = 3$ for the experiment (b)) the β polymorph was observed with a newly reported habit [22]: thin lozenge slabs. Figure 4 shows a picture of a β crystal, with a lozenge habit, observed 210 minutes after the cooling start.

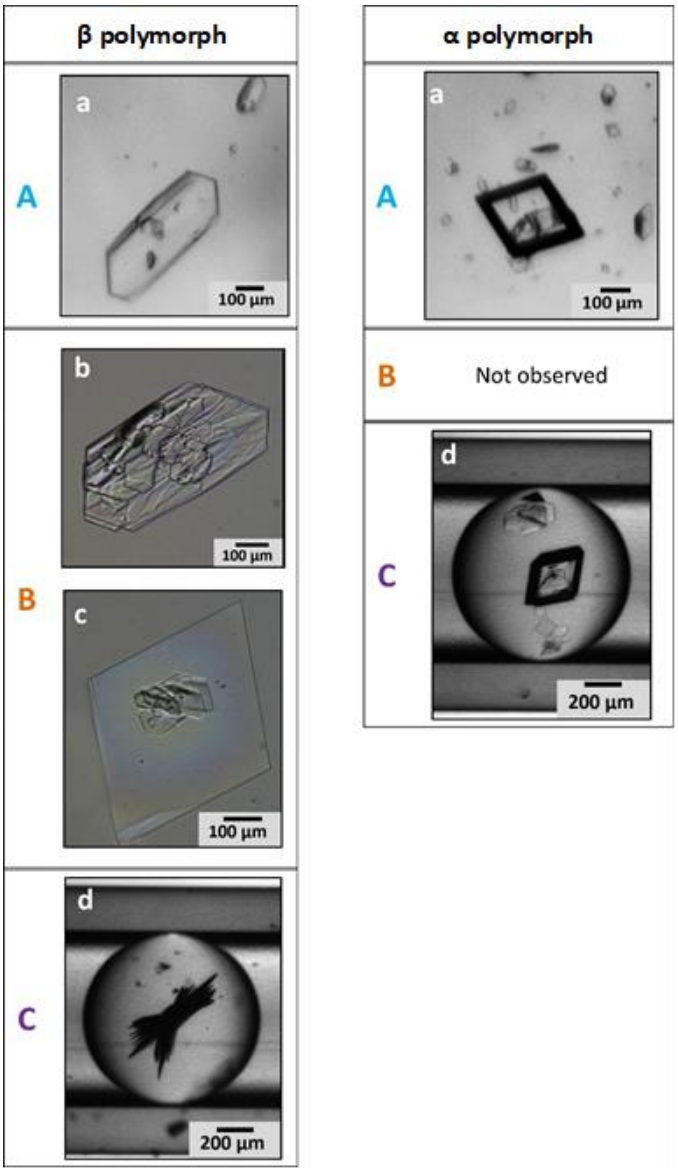

Figure 4. Images of α and β LGlu in: **-A** the 2L Crystallizer: experiment (a) **-B** the 4ml cell: experiments (b) and (c). **-C** The microfluidic device: experiment (d)

-Experiment (d) was carried out in the microfluidic device. 67 droplets with a concentration of 29 g/kg of solvent were generated at 65 °C in a 1 mm capillary. These initial conditions are represented by an empty purple square. The tubing was cooled to 8°C. The nucleation took place after the cooling was achieved and both polymorphs were observed. This is shown by the purple disk (d) in Figure 3. Twenty-four hours after the cooling start, crystals could be observed in 76% of the droplets. The polymorph α was present in 20% of these droplets while β was

observed in 90% of these droplets. The sum of the two percentages exceeds 100% since both polymorphs were observed in 10% of the droplets having crystals inside. Figure 4 shows two droplets observed 24 hours after the start of the cooling. Note that in the picture showing the α polymorph, small crystals of β can also be observed. However, this droplet was tracked for an additional 24 hours and no phase transition was observed. The crystals obtained by microfluidic shown in Figure 4 were also analyzed by Raman spectroscopy.

In the 2L crystallizer, both polymorphs crystallized except for one experiment where the supersaturation was very low according to α solubility ($S_\beta = 1.5$; $S_\alpha = 1.1$). In that latter case, only stable polymorph β was observed (blue Full square in Figure 3). When the supersaturation was sufficient to overcome the thermodynamic advantage of the stable polymorph β, the metastable polymorph α crystallized preferentially at low temperature (between 5°C and 30°C). However, higher temperatures promoted the β polymorph. Moreover, at the conditions where the α polymorph was advantageous (experiences marked: mostly α in Figure 3), the proportion of the β crystals was under 1% (no detection of the presence of β crystals by XRD analysis but few crystals were seen with the video probe). Thus, it can be inferred that LGlu obeyed the Ostwald rule of stages at low temperatures in the 2L stirred crystallizer. In the 4 mL stagnant cell, for all the operating conditions investigated, only the stable polymorph β crystallized with different habits depending on the supersaturation. In the microfluidic device, the stable polymorph β was present in more than 50% of the droplets where nucleation occurred (considering all the experiments); this percentage reached 100% at low supersaturation.

To summarize, the key factors ruling the polymorphic competition, kinetics (ORS) or thermodynamics, differs with the device size and dynamics: the system follows the ORS in the 2L stirred crystallizer at low temperature; thermodynamics governs the process in the 4ml stagnant cell and a kinetic or a thermodynamic control is observed in microfluidics, from one drop to the other.

Previous studies have shown the kinetic advantage (higher growth and nucleation rates) of the metastable polymorph α compared to the stable polymorph β in a stirred medium at low temperatures [21,25–27]. This kinetic advantage was suggested to explain the preferential crystallization of the metastable polymorph α at low temperatures in the stirred crystallizer. However, using only the nucleation and the growth kinetics to explain that the solid phase produced in the stirred crystallizer at low temperature contained less than 1% of the stable polymorph β is not enough, because it forces to consider nucleation and growth rates of β to values unreasonably small. These small values are impossible to be explained physically since the difference in physicochemical properties between the stable and the metastable polymorphs of LGlu are not compatible with such a big difference in the kinetics. In other terms, considering the physical properties of both polymorphs, and especially the interfacial energies that can be deduced from the solubility data for instance, the nucleation kinetics of the stable polymorph cannot be low enough (with respect to that of the metastable polymorph) to avoid the appearance of a significant number of stable polymorph crystals, which should then induce a phase transition leading to only stable polymorph crystals. Therefore, we suggest taking into consideration over solubility of small crystals resulting from the Gibbs Thomson effect to fully explain the results in the 2L stirred crystallizer, i.e. the almost total inhibition of the stable polymorph nucleation, at low temperature, when the Ostwald rule of stages is followed. The influence of the Gibbs Thomson effect is highlighted using the kinetic model presented in the following section.

3. MODELING SECTION:

3.1 Model:

The crystallization of LGlu polymorphs was modeled with taking into account: nucleation, growth and the ripening mechanism resulting from the solubility dependence on size. The supersaturated solution was composed of solvent molecules and LGlu molecules. The LGlu

molecules were treated as monomers. The mechanisms of nucleation, growth, and ripening were modeled through the attachment and detachment of these monomers. Each LGlu polymorph has its own attachment and detachment frequencies as shown in Figure 5.

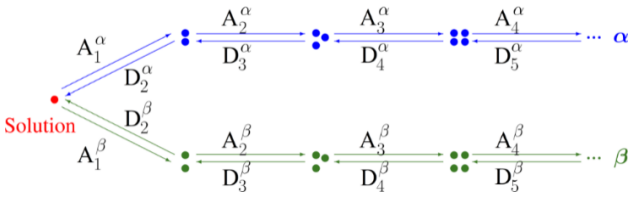

Figure 5. Mechanisms of monomer attachment (A) and detachment (D) to polymorph α and β clusters

Using the attachment and detachment mechanisms, the kinetic equation can be written as follows [28 29]:

$$\frac{dF_i^{\kappa}(t)}{dt} = A_{i-1}^{\kappa} * F_{i-1}^{\kappa} - (A_i^{\kappa} + D_i^{\kappa}) * F_i^{\kappa} + D_{i+1}^{\kappa} * F_{i+1}^{\kappa} = J_{i-1}^{\kappa} - J_i^{\kappa} \quad \text{for } i > 1\,, \tag{1}$$

where:

$$J_i^{\kappa} = A_i^{\kappa} F_i^{\kappa} - D_{i+1}^{\kappa} F_{i+1}^{\kappa}\,, \tag{2}$$

i denotes the number of monomers forming the cluster, κ denotes the α or the β polymorph, $F_i^{\kappa}(t)$ is the number of clusters formed by i monomers per unit mass at time t (kg^{-1}), A_i^{κ} (D_i^{κ}) is the attachment (detachment) frequency of monomers to the i-sized cluster (s^{-1}), and J_i^{κ} is the number of i-sized clusters formed per unit volume per second (kg^{-1} s^{-1}). J_i^{κ} is a general formulation of the nucleation rate[20,29]. Let us note that this denomination is abusive since the term nucleation should be limited to clusters of size larger than the critical size ($i = i_c^{\kappa}$).

In the standard nucleation model, the number of molecules in solution, N_1, does not change in time and thus supersaturation remains unchanged and nucleation is stationary. In contrast with the standard model, the decrease in supersaturation of solution during phase transition is taken into account via the following boundary condition [20]:

$$N_1(t) = N_1(t=0) - [\sum_{i>1} i\, F_i^{\alpha}(t) + \sum_{i>1} i\, F_i^{\beta}(t)]$$

The expression of the attachment and detachment frequencies are given in a previous work[20]. In the calculation of these frequencies for each polymorph, we took into account the following points which exhibit four main differences between α and β LGlu:

-The shape: the clusters were considered as having the same shape as the unit cell

-The solubility: each polymorph solubility was measured in a previous work[22] and was taken into account in the model

-The interfacial energy: in order to fix reasonable values of interfacial energies for each polymorph, we compared different values of interfacial energies. Some of these values were based on correlations between the solubility and the interfacial energy [30–32]. Others were calculated using nucleation data[25]. The interfacial energy values for α and β deduced from a comparative study[20] and used in the simulations are: $\sigma^{\alpha} = 0.013\ (J.m^{-2})$ and $\sigma^{\beta} = 0.014\ (J.m^{-2})$.

-The growth rate: the expression of the attachment and detachment frequencies incorporate a kinetic barrier that may be inferred from the growth rate[20]. The growth rate of each polymorph was deduced from other works [27,33] and was used in the calculations.

3.2 Modeling results:

As shown in the experimental section, in the stirred crystallizer, LGlu obeyed the Ostwald rule of stages at low temperatures. Therefore, to explain the Ostwald rule of stages using the dissolution resulting from the Gibbs Thomson effect, we present in this section the result of simulations done at low temperature. The parameters of the model, as well as the boundary conditions, were given in a previous work [20]. It is worth noting that supersaturation depletion was taken into account. We considered that the nucleation occurred at the final temperature, as observed experimentally. Thus, the simulations were done at a constant temperature (final temperature) equal to 5°C. The initial concentration used in the model was 20.5 (g/kg of

solvent). At 5°C, this concentration corresponded to a supersaturation ratio of 4.22 according to α solubility and 5.59 according to β solubility.

To track the evolution of supercritical clusters (with a size above the critical size) of each LGlu polymorph, we introduced a crystallization fraction X_c^{κ} defined as follows:

$$X_c^{\kappa} = \frac{\sum_{i \geq ic} i\, F_i^{\kappa}}{N_T} \quad . \tag{3}$$

Above, i_c is the critical size and N_T is the total number of LGlu monomers in the system (even those forming the crystals).

Figure 6 depicts the crystallization fraction of each LGlu polymorph as a function of time. It is shown that, at the early stages of the formation of the clusters, the number of supercritical clusters of both polymorphs increased then reached a maximum. However, after less than 0.1s, the number of supercritical clusters of the stable polymorph went down to zero. Also, the number of supercritical clusters of the metastable polymorph α underwent a small decrease, then stabilized in a nonzero value. These simulations showed a fundamental result: the few stable clusters that had nucleated disappeared after 0.1s.

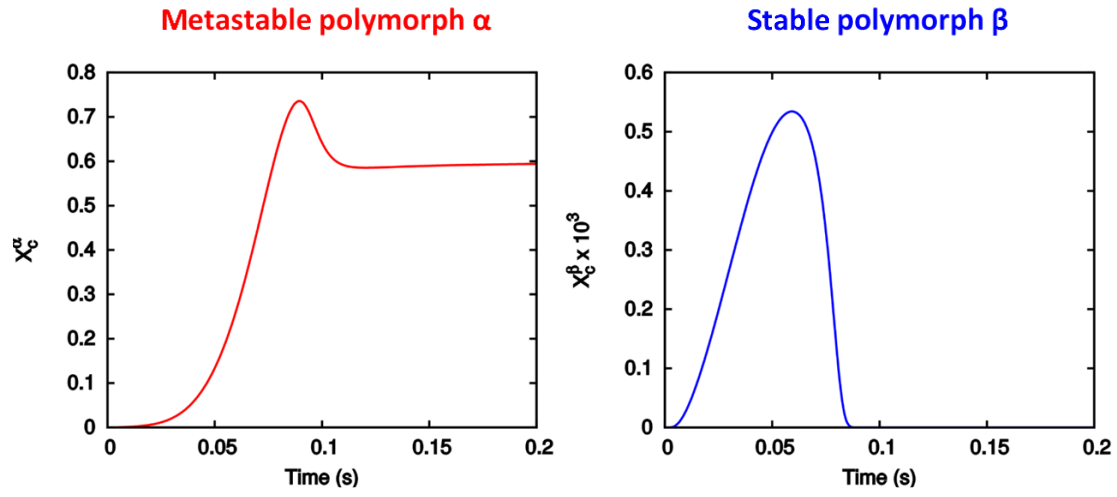

Figure 6. Time evolution of the crystallization fractions X_c^{α} of α LGlu and X_c^{β} of β LGlu

To explain how the stable clusters can vanish, the dimensionless nucleation rate of the clusters was studied. The dimensionless nucleation rate is the nucleation rate (cf. equation (2)) scaled

by its stationary value J^s which corresponds to the nucleation rate at constant supersaturation and temperature [20] (standard nucleation model).

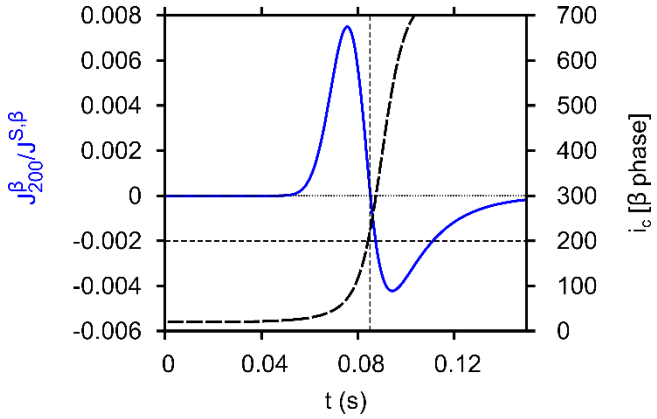

Figure 7. Evolution with time of the dimensionless nucleation rate of polymorph β and of the critical size of its nuclei. Solid line: dimensionless nucleation rate of clusters composed of 200 monomers. Dashed line: critical size

Figure 7 shows how the nucleation rate of β clusters formed by 200 monomers evolved with time. The size of 200 monomers was chosen as an example to demonstrate the variation of the nucleation rate with time. The dimensionless nucleation rate was represented along with the critical size. As demonstrated in the figure, the rate of formation of the clusters increased to a maximum then decreased to a negative value and finally became null. At first sight, this may look unexpected. How can the nucleation rate be negative? In fact, the nucleation rate as defined in equation (2) became negative when detachment term ($D^{\beta}_{i+1}\ F^{\beta}_{i+1}$) became greater than the attachment term $A^{\beta}_{i}F^{\beta}_{i}$. As a result, a dissolution process took place. This dissolution was related to the augmentation of the critical size due to the supersaturation drop during nucleation[34]. Thus, when the critical cluster size reached exactly 200, the dimensionless nucleation rate of β polymorph clusters of size 200 became null (see the dashed intercept on the X-axis). Then, as the critical size continued to increase, the clusters of size 200 became under-saturated and dissolved. This dissolution mechanism due to the concentration depletion during nucleation is

an original ripening mechanism, occurring between two different polymorphs. Indeed, the concentration depletion is mainly due to the α polymorph nucleation and growth. It is noteworthy that the modeling describes the very earlier stages of polymorphs nucleation: the disappearance of the β clusters in the figure 7 takes less than 0.15 seconds and these clusters are smaller than 10nm. These phenomena cannot be directly observed experimentally and the experiments exhibit only the consequences of such mechanism: in the experimentation performed with the stirred crystallizer, the crystals are observed using the video probe once they reach 10µm, a few minutes after establishing the final supersaturation.

4. DISCUSSION:

Unlike the classical population balance model, the kinetic model is a model that "naturally" incorporates the Gibbs Thomson effect by taking into account a critical size that depends on the supersaturation and by using a nucleation rate based on attachment and detachment frequencies. This nucleation description allows the supercritical clusters of the different polymorphs to grow and the under-critical clusters of the different polymorphs to dissolve.

The results of the kinetic model showed in the previous section demonstrated clearly the dissolution of the stable polymorph. Also, they showed that the metastable polymorph took the advantage at the first stages of the crystallization. The qualitative results of the model were in accordance with the experimental results that showed the preferential crystallization of the metastable polymorph at a low temperature (5°C) in the 2L stirred crystallizer. Moreover, let us mention that this model was also able to reflect the behavior of LGlu polymorphs at other temperatures as reported in the reference [20]. These results are fully in agreement with our kinetic explanation of the Ostwald rule of stages, based on an original ripening mechanism occurring between the different polymorph clusters. In the early stages of the crystallization, at the nano-metric scale, both polymorphs nucleate at the same time. However, due to the fast growth of the metastable phase clusters that consume supersaturation, the slow-growing clusters of the

stable polymorph will find themselves undersaturated and will dissolve. This behavior is illustrated in Figure 8. Consequently, in the cases where the difference in growth kinetics between polymorphs is high while their equilibrium concentrations are close, the Gibbs Thomson effect can favor the crystallization of the metastable polymorph to the detriment of the stable polymorph, thus leading to the macroscopic observation of the ORS. Simulations, performed in a previous work[20], gave an order of magnitude of the respective critical sizes of each polymorph: it was found that α critical size increased from 22 monomers (equivalent to 1.8nm) to more than 5000 monomers (equivalent to 11.1nm), while for β stable polymorph, i_c increased from 20 monomers (equivalent to 2.9nm) to more than 700 (equivalent to 9.4nm).

Obviously, transport kinetics between clusters was enhanced in stirred vessel by comparison with stagnant medium. Thus, this ripening mechanism occurring between polymorphs, as the classical Ostwald ripening, was favored by agitation and that is why it was suspected to take place in our experiments performed with the 2L stirred vessel

In the stagnant cell, the mass transfer, ensured by diffusion and thermal convection solely, was slower than in a stirred medium. The nucleation and growth kinetics were then slower. But, above all, the ripening mechanism should have been almost inhibited. Consequently, both polymorphs had more chances to be observed in the unstirred medium, since the dissolution of β nuclei in favor of α nuclei could not occur. In our experiments, only the stable polymorph was formed, even under conditions which led to crystallization that followed the Ostwald rule of stages in the 2L stirred vessel. This result may be due to the high surface to volume ratio of the stagnant cell, which favored heterogeneous nucleation and enhanced the stable polymorph crystallization as suggested in a previous work[35]. Therefore, in the 4ml cell, α lost its kinetic advantage and the β polymorph kept its thermodynamic advantage and crystallized exclusively.

In the microliter droplets, β crystals were predominant but the metastable polymorph α was also observed at high supersaturation. In addition, most of the time, one single polymorphic

phase was present in a given droplet. Our experiments in microfluidics were consistent with observations reported in the literature. Previous studies have stated that, in small volume systems, the probability of observing a metastable polymorph was increased [36–38]. Besides, the α polymorph proportion had been found to decrease with the decreasing supersaturation in a microfluidic device [39], which was also the case in our series of experiments. As in the stagnant cell, the ripening mechanism should be slow in the droplets. However, the stochastic nature of nucleation and the high number of droplets increased the chance of nucleating both polymorphs. Moreover, considering the droplet volume, the first nucleating polymorph was very likely to persist, since it consumed the available supersaturation, limiting other nucleation events. Our experimental results were then coherent, with β polymorph observed in main of the droplets containing crystals, as in the 4mL stagnant cell, but with α polymorph observed in several droplets too.

Among numerous parameters involved in the crystallization of polymorphs, the suggested ripening mechanism occurring between polymorphs appears to play a significant role. This ripening mechanism has some similitudes with Viedma[40] ripening that occurs between chiral crystals. Indeed, one of the key mechanisms behind Viedma Ripening is the Ostwald ripening that leads to the coarsening of the enantiomer with the largest crystals at the expense of the other which causes complete deracemisation[40].

Taking into account the ripening mechanism between polymorphs could be helpful in polymorph screening or in the control of the obtained polymorphic phase in industrial processes. For instance, our experiments performed with setups of different scales showed that microfluidics was an interesting tool for polymorph screening. Indeed, the unstirred and confined medium limited the potential ripening between the polymorph clusters and the phase transition, while the high number of droplets increased the chance of forming all the potential

polymorphic phases. As concern industrial applications, this insight into the Ostwald rule of stages could suggest new routes to control polymorphism.

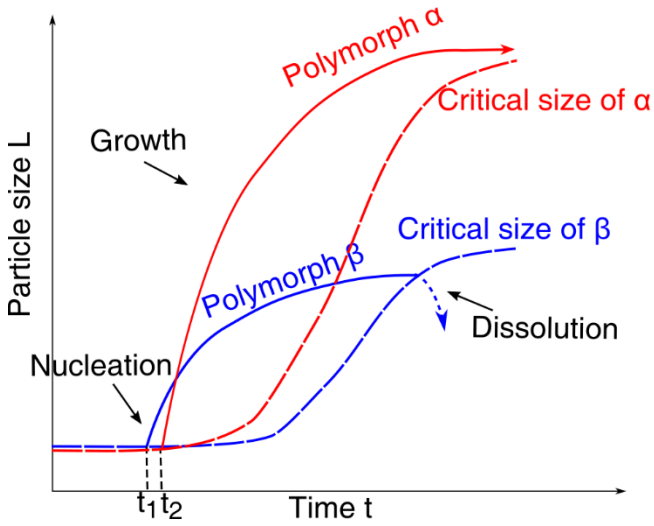

Figure 8. illustration of α and β competition

CONCLUSION

Experiments were performed at different scales, with L-glutamic acid taken as model product. The Ostwald rule of stages was observed in the stirred crystallizer for the experiments performed at low temperature. In a stagnant cell of 4 mL, the stable polymorph was systematically formed. In droplets of around 0.5 µL, produced with a microfluidics device, the stable polymorph β crystallized preferentially or exclusively depending on the supersaturation, with one single phase generally present in a given droplet. This work aimed to interpret these results and suggested to consider an original ripening mechanism occurring between the polymorph nuclei, at the earlier stages of the nucleation, to complete the explanation of the Ostwald rule of stages. This ripening mechanism, due to Gibbs Thomson effect, cannot be introduced in classical modeling solving the population balance equation for the different polymorphs. Conversely, it was "naturally" taken into account by modeling nucleation and growth of the different polymorphs at the earlier stages of crystallization with the kinetic

equation model. Our simulations showed that this ripening mechanism was essential and allowed forcing the nuclei of the stable polymorph to dissolve. In that particular case, i.e. in the 2L stirred crystallizer, the system obeyed the Ostwald rule of stages. Hydrodynamics in the stagnant cell or in the droplets of the microfluidic device was, of course, different from that in the stirred vessel and the ripening mechanism was suspected to be slower. This point, combined with the limited volume of the droplets and the stochastic behavior of nucleation, could explain the results obtained in these two devices.

Besides, this more complete interpretation of the Ostwald rule of stages may suggest new approaches to polymorph screening or control.

ACKNOWLEDGMENTS:

Région Rhône Alpes, France, for supporting the Ph.D. grant of Yousra Tahri

"Crystallize" COST Action CM1402, for supporting the STSM of Yousra Tahri in the Institute of Physics CAS of Prague

Ministry of Education of the Czech Republic for supporting part of this work by the Grant no. LD15004 (VES 15 COST CZ)

REFERENCES:

(1) Bernstein, J. *Polymorphism in Molecular Crystals*; Clarendon Press ; Oxford University Press: Oxford [England]; New York, 2002.

(2) Brittain, H. G. *Polymorphism in Pharmaceutical Solids*; Informa Healthcare: New York, 2009.

(3) Mangin, D.; Puel, F.; Veesler, S. Polymorphism in Processes of Crystallization in Solution: A Practical Review. *Organic Process Research & Development* **2009**, *13*, 1241–1253. https://doi.org/10.1021/op900168f.

(4) Lee, A. Y.; Erdemir, D.; Myerson, A. S. Crystal Polymorphism in Chemical Process Development. *Annual Review of Chemical and Biomolecular Engineering* **2011**, *2*, 259–280. https://doi.org/10.1146/annurev-chembioeng-061010-114224.

(5) Blagden, N.; Davey, R. J. Polymorph Selection: Challenges for the Future? *Crystal Growth & Design* **2003**, *3*, 873–885. https://doi.org/10.1021/cg030025k.

(6) Llinàs, A.; Goodman, J. M. Polymorph Control: Past, Present and Future. *Drug Discovery Today* **2008**, *13* , 198–210. https://doi.org/10.1016/j.drudis.2007.11.006.

(7) Ostwald, W. Z. Studies on Formation and Transformation of Solid Materials. *Z. Phys. Chem* **1897**, *22*, 289–330.

(8) Schmelzer, J. W. P.; Abyzov, A. S. How Do Crystals Nucleate and Grow: Ostwald's Rule of Stages and Beyond. In *Thermal Physics and Thermal Analysis*; Hot Topics in Thermal Analysis and Calorimetry; Springer, Cham, 2017; pp 195–211. https://doi.org/10.1007/978-3-319-45899-1_9.

(9) Nývlt, J. The Ostwald Rule of Stages. *Cryst. Res. Technol.* **1995**, *30*, 443–449. https://doi.org/10.1002/crat.2170300402.

(10) Cardew, P. T.; Davey, R. J. Tailoring of Crystal Growth. In *Conference of the British Association of Crystal Growth, Institute of Chemical Engineers, North Western Branch, Manchester, UK (Inst. Civil Eng., 1982).*; 1982; Vol. 300, p 400.

(11) Parsons, R.; Robinson, K. M.; Twomey, T. A.; Leiserowitz, L.; Roberts, K. J.; Chernov, A. A.; van der Eerden, J. P.; Bennema, P.; Frenken, J. W. M.; Sherwood, J. N.; et al. General Discussion. *Faraday Discussions* **1993**, *95*, 145. https://doi.org/10.1039/fd9939500145.

(12) Van Santen, R. A. The Ostwald Step Rule. *J. Phys. Chem.* **1984**, *88*, 5768–5769. https://doi.org/10.1021/j150668a002.

(13) Threlfall, T. Structural and Thermodynamic Explanations of Ostwald's Rule. *Organic Process Research & Development* **2003**, *7*, 1017–1027. https://doi.org/10.1021/op030026l.

(14) Perez, M. Gibbs-Thomson Effects in Phase Transformations. *Scripta Materialia* **2005**, *52*, 709–712. https://doi.org/10.1016/j.scriptamat.2004.12.026.

(15) Ratke, L.; Voorhees, P. W. *Growth and Coarsening*; Engineering Materials; Springer Berlin Heidelberg: Berlin, Heidelberg, 2002.

(16) Boukerche, M. Cristallisation En Solution d'une Molécule Pharmaceutique : Recherche de Nouveaux Polymorphes. phd, Lyon 1: LAGEP, 2005.

(17) Maggioni, G. M.; Bezinge, L.; Mazzotti, M. Stochastic Nucleation of Polymorphs: Experimental Evidence and Mathematical Modeling. *Crystal Growth & Design* **2017**, *17*, 6703–6711. https://doi.org/10.1021/acs.cgd.7b01313.

(18) Rein ten Wolde, P.; Frenkel, D. Homogeneous Nucleation and the Ostwald Step Rule. *Physical Chemistry Chemical Physics* **1999**, *1*, 2191–2196. https://doi.org/10.1039/a809346f.

(19) Desgranges, C.; Delhommelle, J. Molecular Mechanism for the Cross-Nucleation between Polymorphs. *J. Am. Chem. Soc.* **2006**, *128*, 10368–10369. https://doi.org/10.1021/ja063218f.

(20) Tahri, Y.; Kožíšek, Z.; Gagnière, E.; Chabanon, E.; Bounahmidi, T.; Mangin, D. Modeling the Competition between Polymorphic Phases: Highlights on the Effect of Ostwald Ripening. *Crystal Growth & Design* **2016**, *16*, 5689–5697. https://doi.org/10.1021/acs.cgd.6b00640.

(21) Kitamura, M. Polymorphism in the Crystallization of L-Glutamic Acid. *Journal of crystal growth* **1989**, *96*, 541–546.

(22) Tahri, Y.; Gagnière, E.; Chabanon, E.; Bounahmidi, T.; Mangin, D. Investigation of the L-Glutamic Acid Polymorphism: Comparison between Stirred and Stagnant Conditions. *Journal of Crystal Growth* **2016**, *435*, 98–104. https://doi.org/10.1016/j.jcrysgro.2015.11.019.

(23) Zhang, S.; Ferté, N.; Candoni, N.; Veesler, S. Versatile Microfluidic Approach to Crystallization. *Org. Process Res. Dev.* **2015**, *19*, 1837–1841. https://doi.org/10.1021/acs.oprd.5b00122.

(24) Gerard, C. J. J.; Ferry, G.; Vuillard, L. M.; Boutin, J. A.; Chavas, L. M. G.; Huet, T.; Ferte, N.; Grossier, R.; Candoni, N.; Veesler, S. Crystallization via Tubing Microfluidics Permits Both in Situ and Ex Situ X-Ray Diffraction. *Acta Crystallographica Section F* **2017**, *73*, 574–578. https://doi.org/10.1107/S2053230X17013826.

(25) Lindenberg, C.; Mazzotti, M. Effect of Temperature on the Nucleation Kinetics of α L-Glutamic Acid. *Journal of Crystal Growth* **2009**, *311*, 1178–1184. https://doi.org/10.1016/j.jcrysgro.2008.12.010.

(26) Kitamura, M.; Ishizu, T. Growth Kinetics and Morphological Change of Polymorphs of L-Glutamic Acid. *Journal of crystal growth* **2000**, *209*, 138–145.

(27) Schöll, J.; Lindenberg, C.; Vicum, L.; Brozio, J.; Mazzotti, M. Precipitation of Al-Glutamic Acid: Determination of Growth Kinetics. *Faraday Discussions* **2007**, *136*, 247. https://doi.org/10.1039/b616285a.

(28) Kashchiev, D. *Nucleation Basic Theory with Applications*; Butterworth Heinemann: Oxford; Boston, 2000.

(29) Kožíšek, Z. Crystal Nucleation Kinetics in Confined Systems. *CrystEngComm* **2013**, *15* (12), 2269. https://doi.org/10.1039/c2ce26497h.

(30) Mersmann, A. Calculation of Interfacial Tensions. *Journal of Crystal Growth* **1990**, *102* (4), 841–847. https://doi.org/10.1016/0022-0248(90)90850-K.

(31) Bennema, P.; Söhnel, O. Interfacial Surface Tension for Crystallization and Precipitation from Aqueous Solutions. *Journal of Crystal Growth* **1990**, *102*, 547–556. https://doi.org/10.1016/0022-0248(90)90412-E.

(32) Christoffersen, J.; Rostrup, E.; Christoffersen, M. R. Relation between Interfacial Surface Tension of Electrolyte Crystals in Aqueous Suspension and Their Solubility; a Simple Derivation Based on Surface Nucleation. *Journal of Crystal Growth* **1991**, *113*, 599–605. https://doi.org/10.1016/0022-0248(91)90096-N.

(33) Ochsenbein, D. R.; Schorsch, S.; Vetter, T.; Mazzotti, M.; Morari, M. Growth Rate Estimation of β L-Glutamic Acid from Online Measurements of Multidimensional Particle Size Distributions and Concentration. *Industrial & Engineering Chemistry Research* **2014**, *53*, 9136–9148. https://doi.org/10.1021/ie4031852.

(34) Grossier, R.; Veesler, S. Reaching One Single and Stable Critical Cluster through Finite-Sized Systems. *Crystal Growth & Design* **2009**, *9*, 1917–1922. https://doi.org/10.1021/cg801165b.

(35) Boukerche, M.; Mangin, D.; Klein, J. P.; Monnier, O.; Hoff, C. Inducing the Stable Polymorph Using Heterogeneous Primary Nucleation. *Chemical Engineering Research and Design* **2010**, *88*, 1474–1478. https://doi.org/10.1016/j.cherd.2010.01.027.

(36) Ildefonso, M.; Revalor, E.; Punniam, P.; Salmon, J. B.; Candoni, N.; Veesler, S. Nucleation and Polymorphism Explored via an Easy-to-Use Microfluidic Tool. *Journal of Crystal Growth* **2012**, *342*, 9–12. https://doi.org/10.1016/j.jcrysgro.2010.11.098.

(37) Laval, P.; Giroux, C.; Leng, J.; Salmon, J.-B. Microfluidic Screening of Potassium Nitrate Polymorphism. *Journal of Crystal Growth* **2008**, *310*, 3121–3124. https://doi.org/10.1016/j.jcrysgro.2008.03.009.

(38) Lee, A. Y.; Lee, I. S.; Myerson, A. S. Factors Affecting the Polymorphic Outcome of Glycine Crystals Constrained on Patterned Substrates. *Chemical Engineering & Technology* **2006**, *29*, 281–285. https://doi.org/10.1002/ceat.200500375.

(39) Jiang, N.; Wang, Z.; Dang, L.; Wei, H. Effect of Supersaturation on L-Glutamic Acid Polymorphs under Droplet-Based Microchannels. *Journal of Crystal Growth* **2016**, *446*, 68–73. https://doi.org/10.1016/j.jcrysgro.2016.04.035.

(40) Sögütoglu, L.-C.; E. Steendam, R. R.; Meekes, H.; Vlieg, E.; T. Rutjes, F. P. J. Viedma Ripening: A Reliable Crystallisation Method to Reach Single Chirality. *Chemical Society Reviews* **2015**, *44*, 6723–6732. https://doi.org/10.1039/C5CS00196J.

For table of content use only

Multiscale experimental study and modeling of L-glutamic acid crystallization: emphasis on a kinetic explanation of the Ostwald rule of stages

Yousra Tahri [1,2,6], Emilie Gagnière[1], Elodie Chabanon[1], Tijani Bounahmidi [2,6], Zdeněk Kožíšek[3], Nadine Candoni[4], Stéphane Veesler[4], Moussa Boukerche[5], Denis Mangin[1]

[1]Université de Lyon, Université Claude Bernard Lyon 1, CNRS, UMR 5007, LAGEP, 43 Boulevard du 11 Novembre 1918, 69622 Villeurbanne, France

[2] Euromed Research center, Université Euromed de Fès, Euromed University of Fes, Route de Meknes, 30000, Fès, Morocco

[3] Institute of Physics of the Czech Academy of Sciences, Cukrovarnicka 10, 16200 Praha 6, Czech Republic

[4] CINaM, CNRS, UMR 7325, Aix-Marseille Université, Campus de Luminy, F-13288 Marseille, France

[5] Process Research & Development, AbbVie Inc., 1401 Sheridan Road, North Chicago, Illinois 60064, United States

[6] LASPI, Ecole Mohammadia d'Ingénieurs, Université Mohamed V de Rabat, B.P ; 765 Rabat-Agdal, Morocco

TOC Graphic

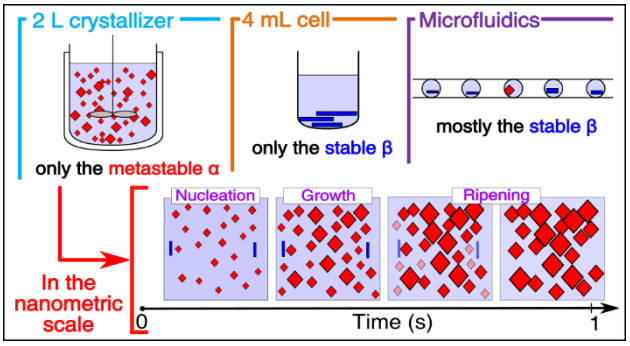

Synopsis

This paper presents an experimental and a modeling study of L-glutamic polymorph crystallization from solution. The experimentation is conducted in a stirred 2L crystallizer, in a stagnant 4ml cell, and in microfluidics. From the results of the experimentation and from the simulations we highlight a kinetic explanation of the Ostwald rule of stage based on the Gibbs Thomson effect.